Metamaterial-enhanced coupling seen as non-Foster impedance matching

Conference Paper · April 2016

CITATIONS
0

READS
31

5 authors, including:

Jorge Virgilio de Almeida
Pontifícia Universidade Católica do Rio de Ja…
3 PUBLICATIONS **0** CITATIONS
SEE PROFILE

Glaucio Siqueira
Pontifícia Universidade Católica do Rio de Ja…
65 PUBLICATIONS **224** CITATIONS
SEE PROFILE

Marco Antonio Grivet Mattoso Maia
Pontifícia Universidade Católica do Rio de Ja…
32 PUBLICATIONS **236** CITATIONS
SEE PROFILE

Carlos Sartori
University of São Paulo
48 PUBLICATIONS **130** CITATIONS
SEE PROFILE

Metamaterial-enhanced coupling seen as non-Foster impedance matching

Jorge V. de Almeida[1,2], Gláucio L. Siqueira[1,2], Marbey M. Mosso[1,2], Marco A. G. M. Maia[1,2], and Carlos A. F. Sartori[3,4]

[1]Center for Telecommunication Studies (CETUC/PUC-RJ), Pontifical Catholic University of Rio de Janeiro, Brazil
[2]Dep. of Electrical Engineering, Center for Science and Technology – Pontifical Catholic University of Rio de Janeiro, Brazil
[3]Nuclear and Energy Research Institute (IPEN/CNEN-SP), University of São Paulo, Brazil
[4]Dep. of Electrical Energy and Automation Engineering, Polytechnic School (PEA/EPUSP) – University of São Paulo, Brazil

KEY WORDS: metamaterial, wireless power transmission, negative inductance, non-Foster impedance matching

SUMMARY

Electrically small antennas (ESA) are characterized by high-Q impedances presenting high reactance and low radiation resistance. Since in most wireless power transmission (WPT) applications, such as inductive power transmission (IPT), to use a full-size antenna is neither practical or desired, the system overall efficiency is usually very poor due to the drivers large reactance. In the last decade, various works have demonstrated that a class of artificial material called metamaterials (MTMs) can synthesize mu-negative (MNG) media capable of evanescent-wave focusing which largely enhances the coupling between ESA. In the present work, MTM-enhanced coupling in IPT systems is examined. Adopting a lumped element approach to describe the general MTM-enhanced IPT system, it is evidenced that MNG media can be interpreted as a negative inductance (a non-Foster reactance) from a circuital point of view. This paper also presents an approach based on energy density to calculate the module of the MNG slab equivalent inductor.

1. INTRODUCTION

Concerning any practical wireless power transmission (WPT) system, three major considerations are usually taken in account: first of all, it must be human and environmentally friendly. Secondly, it may not interfere with other electrical and electronic systems. Finally, it must be efficient enough to be cost-effective compared with traditional transmission lines such as cables.

Once communication systems are mostly far-field based applications, therefore the exploitation of the evanescent waves in the near field for power transfer purpose has gained a lot of interest.

In order to prevent radiation, antennas are made electrically small (ES). Due to high-Q, most of their energy remains stored in their near field and power transfer occurs primarily via induction or tunneling effect, this is to say, evanescent wave coupling. Nonetheless, as it is well-known, IPT systems – consisting in the magnetic coupling between loop antennas – are efficient only for distances smaller than the diameter of the antennas [1].

To diminish such constraints on operating distance, an electromagnetic metamaterial (MTM) presenting effective negative permeability can assist the antennas in order to enhance their magnetic coupling, as demonstrated in [2].

In this paper, a theoretical analysis of the MTM-enhanced coupling phenomenon is presented. From this analysis, a lumped element model for an IPT system assisted by

MTM is proposed. An application of the model is presented in order to illustrate it. The analytical results are confronted with the experimental data.

2. GENERAL THEORETICAL ASPECTS

2.1. Quasistatic field hypothesis

The surrounding space of an antenna is usually subdivided into three theoretical regions: reactive near field, radiating near field (Fresnel region) and far field (Fraunhofer region). However, for an ESA it can be divided into two regions only: the quasistatic field and the radiating field. The theoretical boundary of these two regions is:

$$r = \frac{\lambda_0}{2\pi} \qquad (1)$$

At the radian length r, near field and far field terms are equal. As the near-field zone is a function of the free-space wavelength, it imposes tight limits on the operating frequency of the system.

Whilst in the radiating field the power flows irreversibly away from the source as electromagnetic (EM) radiation, in the quasistatic field one of the oscillating fields dominates the near-field zone and the energy remains stored close to the source, either as electric or magnetic field, seen that Poyting vector is mostly imaginary [3].

One of the virtues of this regime is that almost no energy is lost by the source in the absence of a receiver. Energy starts to flow away only when a proper receptor gets close enough to evanescently couple to the source.

2.2. Foster's reactance theorem

Accordingly to Foster's reactance theorem, the reactance of passive lossless two-terminal networks increase monotonically with frequency [4]. Therefore, the first frequency derivative of a Foster reactance (or susceptance) is *always* positive:

$$X_L = \omega L \rightarrow \frac{d\,X_L}{d\omega} = L,\ if\ L > 0 \qquad (2)$$

$$X_C = -\frac{1}{\omega C} \rightarrow \frac{d\,X_C}{d\omega} = \frac{1}{\omega^2 C},\ if\ C > 0 \qquad (3)$$

Non-Foster impedances are also known as *negative impedances* since their frequency derivative is negative ($L < 0, C < 0$).

2.3. Mu-negative metamaterial as a matching device

Considering that IPT relies on coupled evanescent waves, its efficiency would be greatly improved by "focusing" its evanescent waves. Nonetheless, until quite recently *evanescent-wave focusing* was mostly object of theoretical speculation only. In order to focus evanescent waves they need to be amplified by lenses made from materials presenting negative index of refraction, which have not be found in nature yet. Negative refraction implies that such medium must present both $\varepsilon < 0$ and $\mu < 0$ [5]. In 1999, Pedry published a paper demonstrating that a MNG medium can be artificially achieved

over a limited bandwidth using a 2D-periodical structure made of split-ring resonator unit cells much smaller than their excitation wavelength [6].

Further studies showed that when the EM field is dominated by one of the fields – electric or magnetic – only one of the constitutive parameters, ε or μ, need to be negative in order to focus the evanescent waves [7] [8]. Other studies also showed that spiral resonators present a Q-factor three times higher than a split-ring resonator of the same size and number of turns [9]. So, the considered MTMs in this paper use spiral-resonator based unit cells instead of the split-ring ones.

It is well-known that any sort of interface that produces a discontinuity in the tangent component of the fields supports a surface wave. In the particular case of an interface formed by a MGN slab and a mu-positive (MPS) medium (i.e., the free space) this surface wave is named magnetoinductive (MI) wave [10] [7]. MI waves are *transverse electric* (TE-mode) waves [11]. Since the tangential direction of MNG slabs behave as a perfect electric conductor (PEC) for these TE-mode waves, its transversal direction behaves as perfect magnetic conductor (PMC). Accordingly to Image Theory, the image current induced on a PMC surface has the same orientation of the current flow of the excitation loop which contributes the enhancement of the magnetic flux through the antennas.

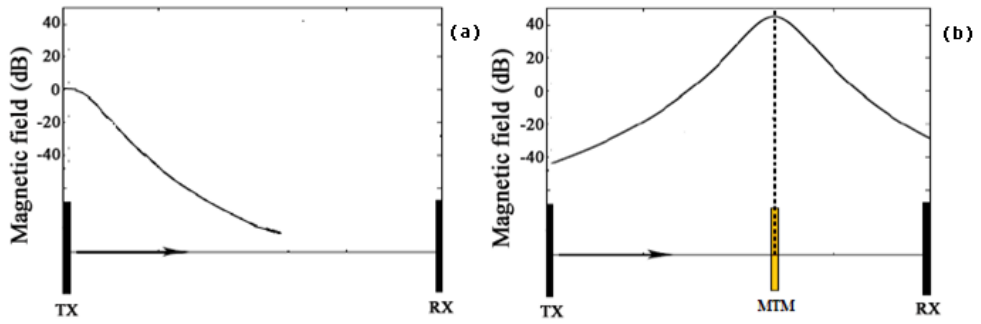

Figure 1. Representation of the magnetic field spatial distribution in the transversal direction for (a) conventional IPT systems and (b) MTM-assisted IPT systems.

Another noticeable fact is that since surface waves are slow ones, this is to say, their *group velocity* is much smaller than *c*. So, the evanescent modes coming from the loop antennas of the IPT system spend more time in the vicinity of the MTM rather than in the vicinity of their source which changes the magnetic field spatial distribution [12]. As shown in Fig. 1 (b), the presence of a MGN slab changes the total reactance felt by the antenna if it is far enough from it.

2.4. Wave propagation in material media

The propagation of an EM wave in space consists in a periodic exchange of energy between the medium and the EM field [13]. The stored energy in the medium on the back side of the wave packet is transformed into field energy and transported to the front side of the wave packet where it is retransformed into stored energy in the medium.

The velocity at which the fields transport energy from the back to the front of the wave packet is known as *phase velocity* v_{phase}. Defining v_{medium} as the velocity of energy transport of the medium (or the rate at which the medium *absorbs* energy), u_{field} as the energy density of the fields and u_{medium} as the energy density of the medium and u as the total energy density, the Poynting vector $\boldsymbol{S}$ can be written as the

energy flux density transported by the fields minus the total energy flux density absorbed by the medium:

$$\boldsymbol{S} = \boldsymbol{v}_{phase} u_{field} - \boldsymbol{v}_{medium} u_{medium} \qquad (4)$$

Averaging over a period, the real part of the $\boldsymbol{S}$ is obtained:

$$\overline{S} = \mathrm{Re}\ \boldsymbol{S} = v_{phase}\overline{u_{field}} - v_{medium}\overline{u_{medium}} \qquad (5)$$

$$\overline{S} \geq 0 \quad (6)$$

The averaging energy flux density $\overline{S}$ can also be expressed in terms of the velocity of the wave packet or *group velocity*:

$$\overline{S} = v_{group}\overline{u} \quad (7)$$

$$v_{phase} = \frac{v_{group}\overline{u} + v_{medium}\overline{u_{medium}}}{\overline{u_{field}}} \qquad (8)$$

Seen that $u = \overline{u_{field}} + \overline{u_{medium}}$:

$$v_{phase} = v_{group} + \frac{(v_{group} + v_{medium})\overline{u_{medium}}}{\overline{u_{field}}} \quad (9)$$

v_{medium} is in general much slower than v_{group}, then it is reasonable to say that:

$$v_{phase} \approx v_{group}\ \left(1 + \frac{\overline{u_{medium}}}{\overline{u_{field}}}\right) = v_{group}\frac{\overline{u}}{\overline{u_{field}}} \qquad (10)$$

In non-dispersive media ($\overline{u_{medium}} = 0$), v_{phase} and v_{group} are exactly the same since the exchange of energy between the medium and the fields is perfectly elastic (the medium absorbs no energy).

$$\overline{u_{medium}} = 0 \rightarrow \overline{u} = \overline{u_{field}} \qquad (11)$$

$$v_{phase} = v_{group} \qquad (12)$$

In normal dispersive media ($\overline{u_{medium}} > 0$), energy is irreversibly absorbed by the medium then v_{phase} exceeds v_{group}:

$$\overline{u_{medium}} > 0 \rightarrow \overline{u} > \overline{u_{field}} \qquad (13)$$

$$v_{phase} > v_{group} \qquad (14)$$

In anomalous dispersive media, dispersion is negative ($\overline{u_{medium}} < 0$). This phenomenon occurs around the absorption resonance of any material medium: v_{group} surpasses *c* in magnitude and loses its physical meaning because the envelope of the wave packets is time-variant. For that reason, the velocity of energy transport not in

terms of the *group velocity* but as *signal velocity*, the velocity of the wave front which always equal or smaller than *c* [13].

$$\overline{u_{medium}} < 0 \rightarrow \overline{u_{field}} > \overline{u} \qquad (15)$$

$$v_{group} > v_{phase} > c \qquad (16)$$

In this state, the medium is said to be *excited*. Considering that negative energy density is physically senseless, anomalous dispersion implies that energy flows out of the medium. Instead of net energy density being transported from the wave front into the medium as in normal dispersion (absorption), it is the front wave that *extracts* net energy density from the medium by reducing its excitation. Considering a passive medium in anomalous dispersion, $\overline{S}$ must be zero once the medium cannot supply more power than the power carried by the fields:

$$v_{phase}\overline{u_{field}} = v_{medium}\overline{u_{medium}} \qquad (17)$$

$$v_{phase} = v_{medium}\frac{\overline{u_{medium}}}{\overline{u_{field}}} \qquad (18)$$

$$\overline{u_{medium}} < 0 \rightarrow v_{phase} < 0 \qquad (19)$$

A consideration about negative v_{phase} is that at first glance it seems to imply that energy is being inversely transported from the front side of the wave packet into its back side, which is nonsense. As mentioned above, the wave front is increasing in intensity. Evanescent-mode enhancement is achieved by redistributing energy from lower frequency modes to higher frequency modes. The enlargement of the frequency spectrum compresses the wave-packet width in time increasing its intensity but conserving the total energy it carries. Notice that the real part of the Poynting vector is zero, indicating that the amplification process does not violate energy conservation law [8] [14].

2.5. Energy density and amplification capability of mu-negative metamaterials

In IPT systems assisted by MTM, the energy stored in the MNG slab is transferred to the incident evanescent wave by means of anomalous dispersion. It means that the amplification capability of the MTM is close related to the amount of energy stored in it.

In this work, the unit cell of the considered MTM is a spiral resonator (FIG). Accordingly to [15], the maximum energy density stored in a spiral resonator is given by:

$$u_m = \frac{\mu_0}{2}\ 1 + 2AQ_{cell}^2\ \ H\ ^2\ \ [J/m^3] \quad (20)$$

$$A = \frac{{M_0}^2}{L_0 L_{cell}} \qquad (21)$$

Where Q_{cell} is the quality factor of the unit cell, L_{cell} is its self-inductance, L_0 the self-inductance of the source and M_0 is their mutual inductance.

3. PROPOSED LUMPED ELEMENT MODEL FOR LOSSLESS METAMATERIAL-ENHANCED IPT SYSTEMS

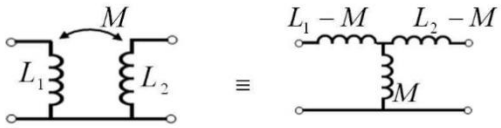

Figure 2. T-circuit transformation.

Assuming that the antennas operate far from self-resonance and doing the complementary hypotheses that the electrical resistance of the wires, the radiative resistance of the antennas and the internal resistance of the source are all negligible, and using the circuit transform identity presented in Fig. 2, the model of an IPT system can be simplified to the one showed in Fig. 3.

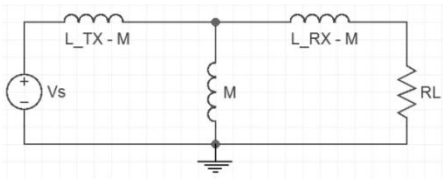

Figure 3. Equivalent lumped element model for lossless IPT systems.

As mentioned above, excited MNG slabs support MI waves that *attract* the magnetic field to the vicinity of the MTM (see Fig. 1). Considering that these waves present an almost inductive behavior since the energy stored in the magnetic field exceeds the energy stored in the electrical field, let's assume the hypothesis that a MNG slab adds a series negative reactive load to the antenna, nor as Foster capacitive susceptance ($C > 0$) once the net stored energy is magnetic, but as a non-Foster inductive reactance ($L < 0$). It is admitted as a negative inductance because the energy is transferred oppositely, from the excited surface of the MTM to the evanescent waves of the system (see section 2.4), hence increasing locally the magnetic potential of the inductive link instead of reducing it as a conventional Foster impedance.

Thus, a MNG slab assisting the transmitting antenna would be perceived as a negative inductance by the transmitter ($L_{MTM,TX} < 0$) while a MNG slab assisting the receiving antenna would be perceived as a negative reactance by the receiver ($L_{MTM,RX} < 0$).

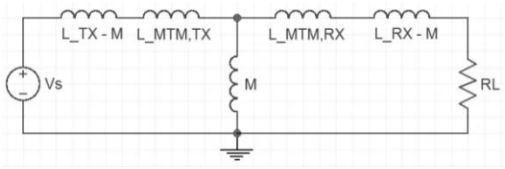

Figure 4. Proposed lumped element model for MTM-enhanced IPT systems.

The proposed lumped element for lossless MTM-enhanced IPT systems is shown in Fig 4. The complete model considers the general case where the antennas are simultaneously assisted by MTM and the MTM are independently coupled to each driver. The total impedance of the proposed model seen from the transmitter Z_1 when the source operates around the resonant frequency ω_0 of the MTM is given by:

$$Z_1\ \omega\ _{\omega=\omega_0} = j\ \frac{\omega^3 L_{RX}^2 L_{TX} - \omega^3 L_{RX}^2\ L_{MTM,TX}\ - 2\omega^3 L_{RX} L_{TX}\ L_{MTM,RX}}{R_L^2 + \omega^2 L_{RX}^2 - 2\omega^2 L_{RX}\ L_{MTM,RX}\ - \omega^2 L_{MTM,RX}^2}$$

$$+j\ \frac{2\omega^3 L_{RX}\ L_{MTM,TX}\ \ L_{MTM,RX}\ - \omega^3 L_{RX} M^2 - \omega^3\ L_{MTM,TX}\ L_{MTM,RX}^2}{R_L^2 + \omega^2 L_{RX}^2 - 2\omega^2 L_{RX}\ L_{MTM,RX}\ - \omega^2 L_{MTM,RX}^2}$$

$$+j\ \frac{\omega^3 L_{TX} L_{MTM,RX}^2 + \omega^3 M^2\ L_{MTM,RX}\ + \omega L_{TX} R_L^2 - \omega\ L_{MTM,TX}\ R_L^2}{R_L^2 + \omega^2 L_{RX}^2 - 2\omega^2 L_{RX}\ L_{MTM,RX}\ - \omega^2 L_{MTM,RX}^2} \qquad (22)$$

$$+\ \frac{\omega^2 M^2 R_L}{R_L^2 + \omega^2 L_{RX}^2 - 2\omega^2 L_{RX}\ L_{MTM,RX}\ - \omega^2 L_{MTM,RX}^2}$$

$$M = \kappa\ \ \overline{L_{RX} L_{TX}} \qquad (23)$$

Where M is the mutual inductance and κ is the coupling coefficient.

$$PTE = \frac{Re\ Z_1}{Z_1} = \frac{1}{1 + j\frac{Im\ Z_1}{Re\ Z_1}} = \frac{1}{1 + jQ_{SIST}} \qquad (24)$$

$$Q_{SIST} \triangleq \frac{Im\ Z_1}{Re\ Z_1} \qquad (25)$$

$$S_{21}(dB) = 10 \log\ PTE \qquad (26)$$

S_{21} is the *power transfer gain* and Q_{SIST} is the *quality factor* of the system defined as the ratio between time-average stored and transmitted energy in the system (which is a measure of line loss per wavelength). So, the condition for maximum PTE is to minimize Q_{SIST}.

4. CALCULATING L_{MTM} FROM ENERGY DENSITY

Knowing that the energy stored in an inductor is:

$$U_m = \frac{L\ I^2}{2} \quad [J] \qquad (28)$$

The MTM equivalent inductance L_{MTM} when operating around ω_0 is related to its energy density through:

$$\frac{L_{MTM}\ I^2}{2} \approx\ N\ \ \frac{\mu_0}{2}\ 1 + 2AQ_{cell}^2\ \ H^{\ 2} = \frac{N\mu_0}{2}\ 1 + 2AQ_{cell}^2\ (volume_{cell})\ H^{\ 2} \qquad (27)$$

Where N is the number of unit cells of the MTM slab that are activated by the excitation loop as shown in Fig. 5. The activated unit cells are supposed to be strongly coupled to the driver (A=1).

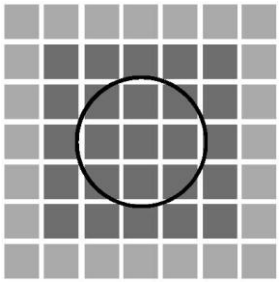

Figure 5. Representation of the driver in front of the MTM slab.

Defining the normalized loop current as

$$I \triangleq \frac{I}{H} \quad [m] \quad (29)$$

A parameter of dimension *meter* comparable in size with the circumference of excitation loop is obtained. Thus, the module of the MTM-equivalent lumped inductor can be estimated by:

$$L_{MTM} = \frac{N\mu_0 \ 1+2Q_{cell}^2}{I^2}(volume_{cell}) \quad [H] \quad (30)$$

5. APPLICATION

In order to validate the proposed model, the analytical results are compared with experimental data. The considered configurations of the MTM-enhanced system are shown in Fig. 6. The MTM synthesizing the MNG slabs is the same model exploited in [2]. It is main characteristics are presented in Table 1.

The transceivers are loops antennas with radius $r = 5cm$, made of 18 AWG copper wire and separated by a distance $d = 15cm$. The load R_L is 50 Ohms. The self-inductance of circular ES antennas is estimated by [16]:

$$L_0 = \mu_0 a \ \ln \frac{8a}{p} - 1.75 = 620\ nH \quad (31)$$

$$L_{TX} = L_{RX} = L_0 \quad (32)$$

Where *a* is the diameter of the antenna and *p* is the diameter of the wire.

The coupling coefficient of the antennas can be estimated by [17]:

$$\kappa = \frac{\mu_0 \pi r^4}{L_0 \ \overline{4r^2+d^2}d^2} = 1 \cdot 10^{-2} \quad (32)$$

$$I = \pi a = 31.6\ cm \quad (33)$$

Admitting that the MTM slabs are identical and are just before the drivers:

$$L_{MTM} = 560\ nH \quad (34)$$

$$G \triangleq S_{21_{MTM-enhanced}} - S_{21_{Ref}} \quad (35)$$

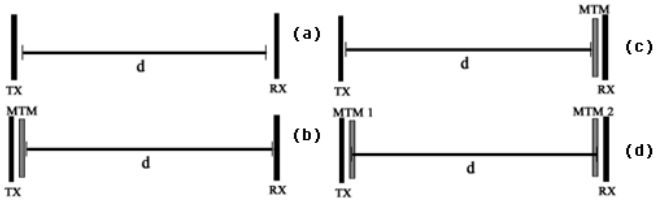

Figure 6. Schematic of the system (a) reference configuration, (b) configuration 1, (c) configuration 2 and (d) configuration 3.

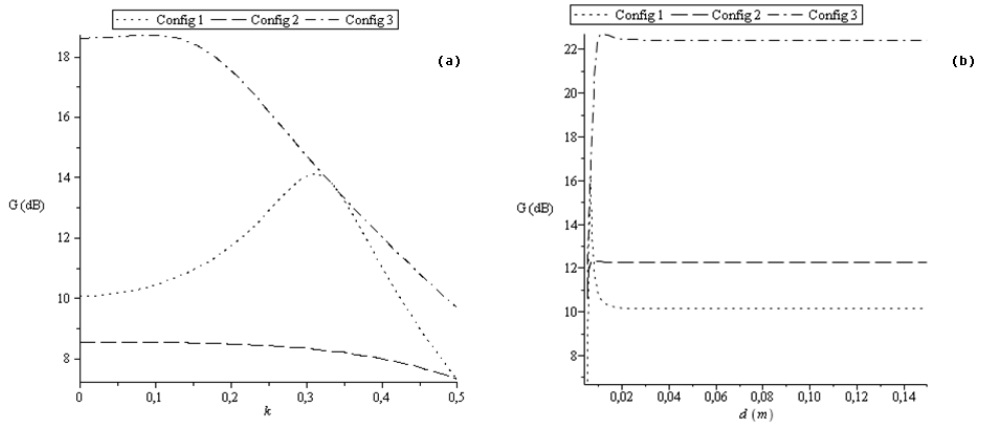

Figure 7. Gain as a function of the coupling coefficient (a) and the distance between the MTM-assisted antennas (b).

Varying the system coupling coefficient by approximating the antennas, the coupling dependence of the gain is evidenced. As shown in Fig. 7, the MTM gain tends to a constant value for very small values of κ (smaller than 0.1) and decays linearly when κ starts to increase.

For greater values of κ greater than 0.3, the estimation of the gain becomes inaccurate for *configuration 3* since the antennas are too close to each other (κ = 0.3 implies d=1.6 cm) hence the hypothesis that the MNG slabs are independently coupled to the drivers are not valid anymore. In this situation, the MTM-enhanced IPT system would be better described by *configuration 1*.

Another important observation concerning *configuration 1* is that there is an optimal coupling that maximizes the gain.

6. EXPERIMENTAL RESULTS AND DISCUSSION

The experimental setup is shown in Fig. 8. The main results obtained for the considered configurations are summarized in Table 3.

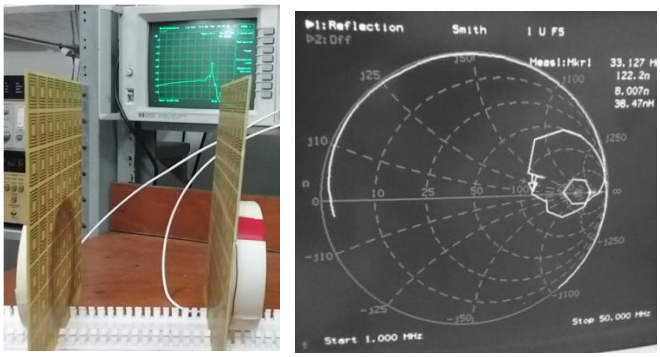

Figure 8. Experimental setup and the Smith chart of the MTM-enhanced IPT system at resonance.

The proposed lumped element model and the experimental measurements achieved very similar results (see Table 2 and 3). Around the operating frequency f_0, the MTM-assisted antennas clearly describes a non-Foster behavior seen that the reactance derivative changes its sign presenting a capacitive response. As shown in Fig. 8, the introduction of a MTM greatly reduces the total reactance of the transmitter (at resonance, the impedance of the transmitter becomes almost resistive).

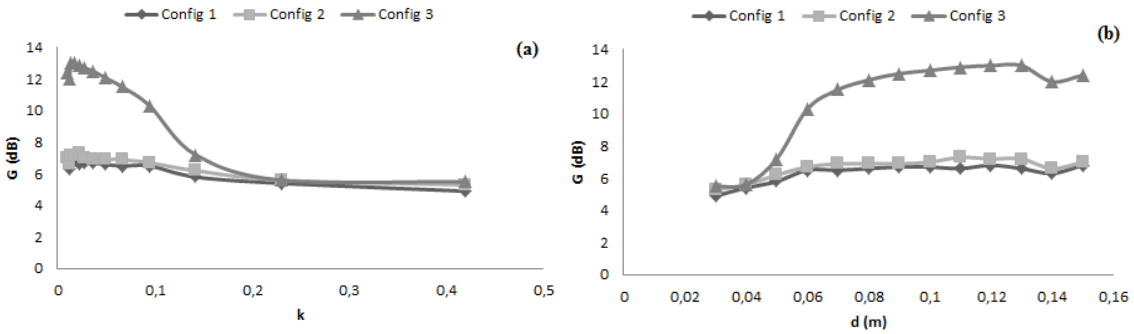

Figure 9. Gain as a function of the coupling coefficient (a) and the distance between the MTM-assisted antennas (b).

Fig. 9 shows that for two loosely coupled antennas assisted by MTM the general behavior is basically the superposition of *configurations 1* and *2*. When the antennas get close, the MTMs interfere with each other behaving as they were one structure. As seen in Fig. 9, *configuration 3* tends to *configuration 1* and *2* when the antennas are strongly coupled. Also, the MTM induced gain degrades when the antennas come close together because mutual inductance and the MTM add both negative phase to the total antenna impedance. When κ tends to unity, the assisted antenna starts to behave more and more capacitively going away from resonance (hence, reducing PTE).

Since the total Q_{SIST} of the inductive link is reduced (see Tables 2) in the presence of a non-Foster reactance, the impedance matching between the drivers improves as a consequence of the reduction of the antenna reactive power. It is important to notice that Q_{SIST} concerns the inductive link not the antennas, thus its reduction does not implicate on improvement of the antenna bandwidth. On the contrary, seen that dispersion is a stability condition of passive structures with negative parameters the net gain occurs over a strict narrow band of frequencies.

Finally, a criterion for maximum transfer is derived from the proposed model. Minimizing Q_{SIST} implies that the module of the negative inductance represented by the MTM must tend to the module of the assisted antenna inductance ($L_{MTM} = L_0$). Since the gain limitation ($L_{MTM} < L_0$) arises from the random phase of MI waves due to material losses [18], an external and active control of the MTM is needed in order to achieve the phase-matching condition for perfect transfer [19].

7. CONCLUSION

A lumped element model for MTM-enhanced IPT systems with associated experimental measurements has been presented. It demonstrates that a MNG slab can be interpreted as a non-Foster reactance in series with the assisted antenna. Besides, the model elucidates the overall gain introduced by the MTM as improved impedance matching due to the reduction of the antenna reactance. Moreover, a methodology to estimate the module of the equivalent negative inductor represented by the MTMs is described. In the future, designers could benefit from this concept as an optimization parameter for WPT system based on inductive coupling.

REFERENCES

[1] D. v. Wageningen and E. Waffenschmidt, "Wireless Power Consortium," [Online]. Available: http://www.wirelesspowerconsortium.com/technology/transfer-efficiency.html. [Accessed 29 1 2016].

[2] S. I. Nishimura, J. V. de Almeida, C. Vollaire, C. A. F. Sartori, A. Breard, F. Morel and L. Krähenbühl, "Enhancing the inductive coupling and efficiency of wireless power transmission system by using metamaterials," in *16th SBMO and 11th CBMag*, Curitiba, 2014.

[3] H. A. Haus and J. R. M. , Electromagnetic Fields an Energy, Prentice Hall, 1989.

[4] R. Foster, "A Reactance Theorem," *Bell System Technical Journal,* 1926.

[5] V. G. Veselago, "The electrodynamics of substances with simultaneously negative valus of epslon and mu," *Soviet Physics Uspekhi,* vol. 10, no. 4, 1968.

[6] J. B. Pendry, A. J. Holden, D. J. Robbins and W. J. Stewart, "Magnetism from Conductors and Enhanced Nonlinear Phenomena," *IEEE Transactions on Microwave Theory and Techniques,* vol. 47, no. 11, 1999.

[7] F. Capolino, Theory and Phenomena of Metamaterials, CRC Press, 2009.

[8] N. Engheta and R. W. Ziolkowski, Electromagnetic Metamaterials: Physics and Engineering Explorations, Wiley-IEEE Press, 2006.

[9] F. Bilotti, A. Toscano and L. Vegni, "Design of Spiral and Multiple Split-Ring Resonators for the Realization of Miniaturized Metamaterial Samples," *IEEE Transactions on Antennas and Propagation,* vol. 55, no. 8, 2007.

[10] R. W. Ziolkowski and N. Engheta, Electromagnetic Metamaterials: Physics and Engineering Explorations, Wiley-IEEE Press, 2006.

[11] E. Shamonina, "Magnetoinductive polaritons: Hybrid modes of metamaterials with interelement coupling," *Physical Review B,* no. 85, 2012.

[12] F. Capolino, Applications of Metamaterials, CRC Press, 2009.

[13] L. Brillouin, Wave propagation and group velocity, New York and London: Academic press, 1960.

[14] J. A. B. Faria and M. P. Pires, "Theory of Magnetic Transmission Lines," *IEEE TRANSACTIONS ON MICROWAVE THEORY AND TECHNIQUES,* vol. 60, no. 10, 2012.

[15] S. Tretyakov, "Electromagnetic field energy density in artificial microwave materials with

strong dispersion and loss," *Physics Letters A,* vol. 343, p. 231–237, 2005.

[16] "Antenna Theory," [Online]. Available: http://www.antenna-theory.com/antennas/smallLoop.php. [Accessed 29 01 2016].

[17] R. M. Duarte and G. K. Felic, "Analysis of the Coupling Coefficient in Inductive Energy Transfer Systems," *Hindawi Publishing Corporation,* no. Active and Passive Electronic Components, 2014.

[18] E. Shamonina and L. Solymar, Waves in Metamaterials, Oxiford, 2009.

[19] I. V. Shadrivov, M. Lapine and Y. S. Kivshar, Eds., Nonlinear,tunable and active metamaterials, Springer, 2015.

TABLES

MTM parameters	
L_{cell}	$846nH$
f_0	$33\ MHz$
$C = \frac{1}{\omega_0^2 L}$	$100pF$
Q_{cell}	180
N	49

Table 1. The constitutive parameters of the MTM slab.

Analytical results			
	$Q_{SIST}\ (dB)$	$S_{21}\ (dB)$	$G\ (dB)$
Ref.	*44.7*	*-44.7*	---
Config. 1	*34.6*	*-34.6*	*10.1*
Config. 2	*36.2*	*-36.2*	*8.5*
Config. 3	*26.1*	*-26.1*	*18.6*

Table 2. Analytical results from the proposed model.

Experimental results		
	$S_{21}\ (dB)$	$G\ (dB)$
Ref.	*–38.8*	---
Config. 1	*–32*	*6.8*
Config. 2	*–31.8*	*7*
Config. 3	*–26.4*	*12.4*

Table 3. Experimental results of the considered configurations.